BULLETIN OF THE CHEMICAL SOCIETY OF JAPAN VOL. 41 920—928 (1968)

Kinetic Study of the Gas-phase Oxidation of Propylene in a Propylene-excess Atmosphere under Pressure*[1]

Mitsuo MASAI, Etsuro ECHIGOYA*[2] and Kiyoshi MORIKAWA

Research Laboratory of Resources Utilization, Tokyo Institute of Technology, Ookayama, Meguro-ku, Tokyo

(Received March 16, 1967)

Reaction-rate equations are derived for oxygen, acetaldehyde, propylene oxide, carbon monoxide, and ethylene on the basis of a plausible reaction scheme. These rate equations are shown to fit the experimental results obtained using a flow-type reactor. It seems most reasonable to conclude that the above reaction mechanism is correct. The type of flow of the reactant gas through the reactor used in this work can be practically regarded as a plug flow from the measurements of the resisdence time distribution using the pulse-tracer method.

In our earlier papers dealing with the gas-phase oxidation of propylene in a propylene-excess atmosphere under pressure using an inert fluidized bed reactor, it was shown that the formations of oxygenated products, such as acetaldehyde and propylene oxide, were favored in a propylene-excess atmosphere,(1) and a plausible reaction scheme was presented which fit the experimental results obtained well.(2)

The purpose of the present paper is to discuss kinetically the reaction scheme reported earlier.(2) It is necessary to obtain a reaction scheme which can elucidate all the main phenomena accompanying this reaction. The reaction scheme proposed in the previous paper(2) fit well the experimental results obtained there. However, because of the complexity of the reaction system, and also because of the lack of other suitable analytical methods, the kinetic study is still a powerful method by which to ascertain what is proceeding in the reaction system predominantly. Among the several papers published concerning the kinetic study of the oxidation of propylene,(3) only Kamiya, Sekine and Yamakawa employed a flow method; they showed that the rate of oxygen consumption is first-order with relation to the concentration of oxygen at the total pressures of 4 and 6 atm, and also that the rate constant in this rate equation is proportional to the -0.75th power of the surface area of the reactor wall.(4)

The flow-type reactor is considered to be suitable for use in following a rapid reaction. The residence-time distribution in the reactor was measured by means of the pulse-tracer technique;(5) the residence time distribution in the reactor used here is practically neglected in the experimental region, so the correct reaction time in this flow reactor can be easily calculated.

On the basis of the reaction scheme reported earlier by the present authors,(2) the reaction-rate equations for the initial reaction step are derived for oxygen, acetaldehyde, propylene oxide, carbon monoxide, and ethylene, the major components in this reaction system. These equations demonstrably fit the experimental results obtained here well. Therefore, it seems most reasonable to conclude that the proposed mechanism of the reaction is correct.

Experimental

Materials. The propylene gas and oxygen have been described before.(1)

Apparatus. The kinetic experiments were carried out in a usual flow-type reactor, 14.8 mm i. d. × 803 mm length and made of stainless steel*[3]; the reactor was mounted vertically, as shown in Fig. 1. The pressure in the reactor was controlled by a needle valve of stainless steel*[3] at the bottom of the the reactor. The inner surface of the reactor was polished nearly to a mirror surface, and the reactor was heated from outside by a fused metal bath.

Procedures. The kinetic experiments were carried out in the region of the low conversion of oxygen;

---

*[1] Part of this paper was presented at the 19th Annual Meeting of the Chemical Society of Japan, Tokyo, April, 1966.

*[2] Present address: Department of Chemical Engineering, Faculty of Engineering, Tokyo Institute of Technology.

1) E. Echigoya, M. Masai and K. Morikawa, This Bulletin, **41**, 904 (1968).

2) M. Masai, E. Echigoya and K. Morikawa, *ibid.*, **41**, 910 (1968).

3) V. Ya. Shtern, "The Gas-Phase Oxidation of Hydrocarbons," translated by M. F. Mullins, Pergamon Press, Oxford (1964), pp. 527—573.

4) Y. Kamiya, N. Sekine and Y. Yamakawa, *Sekiyu Gakkai Shi (J. Japan Petrol. Inst.)*, **8**, 951 (1965).

5) T. Miyauch, "Ryukei-Sosa To Kongo-Tokusei" (Operation of a Flow System and Characteristics of Mixing Phenomena), Zoku Shin Kagaku Kogaku Koza, Vol. 14, Nikkan Kogyo Shinbunsha Co., Tokyo (1962), p. 16.

*[3] JIS SUS 32, AISI 316, Austenite

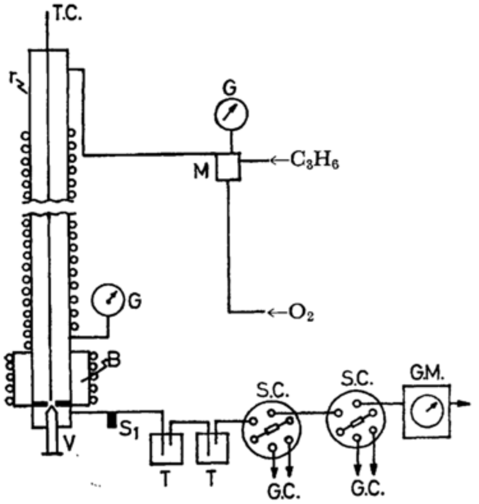

Fig. 1. Flow sheet of reaction apparatus.
B, fused metal bath; G, press. guage (Bourdon type); G. C., gas chromatograph; G. M., wet gas meter; M, gas mixer; r, reactor; S_1, sampling point; S. C., sampling cock; T, cold trap; T.C., thermocouple; V, press. control valve

i. e., the assumption of differential reactor nearly holds. The part of the reactor with temperatures higher than 360°C was regarded as a reaction space, on the basis of previously obtained results.[2] The volume change in the reaction was $+3$—-4.9%, therefore, the volume change during the reaction was neglected. The temperature distributions through the reactor were similar for the same mean reaction temperatures. The mean reaction temperatures were evaluated by averaging the temperatures measured at 5—10 mm intervals along the gas flow with equation, $T_{\text{aver}}=(\sum T_i\times l_i)/(\sum l_i)$, where T_i is the measured temperature and l_i is the distance from the bottom of the reactor to the point where T_i was measured. The reaction rates were evaluated carefully from the gradient of the concentration *vs.* reaction time curves (Figs. 3—5, 7—12).

Analysis. The procedure was that described for Exp. B in an earlier paper.[2]

Rate Equations

The reaction scheme which was discussed in the earlier paper[2] was as follows:

0 $CH_2{=}CH{-}CH_3 + O_2 \rightarrow CH_2{=}CH{-}\dot{C}H_2 + HO\dot{O}$

1 $CH_2{=}CH{-}\dot{C}H_2 + O_2 \rightarrow CH_2{=}CH{-}CH_2O\dot{O}$

2a $CH_2{=}CH{-}CH_2O\dot{O} + C_3H_6 \rightarrow$
$CH_2{=}CHCH_2OOCH_2\dot{C}HCH_3$

2b $CH_2{=}CHCH_2OOCH_2\dot{C}HCH_3 \rightarrow$
$CH_2{=}CHCH_2OO\dot{C}HCH_2CH_3$

2c $CH_2{=}CHCH_2O\dot{O} + C_3H_6 \rightarrow$
$CH_2{=}CHCH_2OOH + CH_2{=}CH\dot{C}H_2$

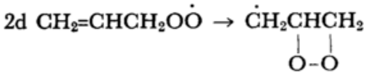
2d $CH_2{=}CHCH_2O\dot{O} \rightarrow \underset{\dot{O}-\dot{O}}{\dot{C}H_2CHCH_2}$

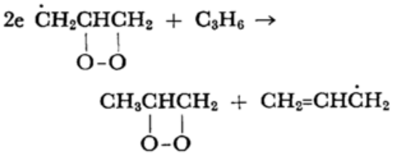
2e $\underset{\dot{O}-\dot{O}}{\dot{C}H_2CHCH_2} + C_3H_6 \rightarrow$
$\underset{\dot{O}-\dot{O}}{CH_3CHCH_2} + CH_2{=}CH\dot{C}H_2$

2f $CH_2{=}CHCH_2O\dot{O} \rightarrow CH_2{=}CH\dot{C}HOOH$

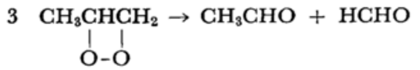
3 $\underset{\dot{O}-\dot{O}}{CH_3CHCH_2} \rightarrow CH_3CHO + HCHO$

4a $CH_3CHO + O_2 \rightarrow CH_3\dot{C}O + HO\dot{O}$

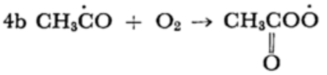
4b $CH_3\dot{C}O + O_2 \rightarrow CH_3\underset{\overset{\|}{O}}{C}O\dot{O}$

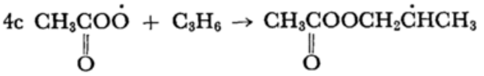
4c $CH_3\underset{\overset{\|}{O}}{C}O\dot{O} + C_3H_6 \rightarrow CH_3\underset{\overset{\|}{O}}{C}OOCH_2\dot{C}HCH_3$

5a $CH_3\dot{C}O \rightarrow \dot{C}H_3 + CO$

5b $CH_3\dot{C}O + C_3H_6 \rightarrow CH_3CHO + CH_2{=}CH\dot{C}H_2$

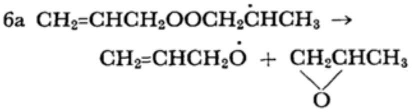
6a $CH_2{=}CHCH_2OOCH_2\dot{C}HCH_3 \rightarrow$
$CH_2{=}CHCH_2\dot{O} + \underset{\diagdown O \diagup}{CH_2CHCH_3}$

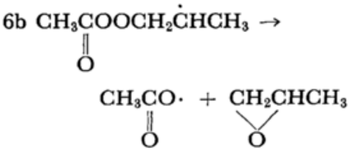
6b $CH_3\underset{\overset{\|}{O}}{C}OOCH_2\dot{C}HCH_3 \rightarrow$
$CH_3\underset{\overset{\|}{O}}{C}O\cdot + \underset{\diagdown O \diagup}{CH_2CHCH_3}$

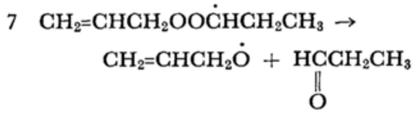
7 $CH_2{=}CHCH_2OO\dot{C}HCH_2CH_3 \rightarrow$
$CH_2{=}CHCH_2\dot{O} + H\underset{\overset{\|}{O}}{C}CH_2CH_3$

8 $CH_2{=}CHCH_2OOH \rightarrow CH_2{=}CHCHO + H_2O$

9 $CH_2{=}CH\dot{C}HOOH \rightarrow CH_2{=}\dot{C}H + CO + H_2O$

10 $CH_2{=}CHCH_2\dot{O} \rightarrow CH_2{=}\dot{C}H + HCHO$

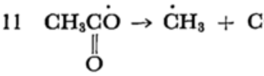
11 $CH_3\underset{\overset{\|}{O}}{C}\dot{O} \rightarrow \dot{C}H_3 + CO_2$

12 $CH_2{=}\dot{C}H + C_3H_6 \rightarrow CH_2{=}CH_2 + CH_2{=}CH\dot{C}H_2$

13 $\dot{C}H_3 + C_3H_6 \rightarrow CH_4 + CH_2{=}CH\dot{C}H_2$

14 $HO\dot{O} + C_3H_6 \rightarrow HOOH + CH_2{=}CH\dot{C}H_2$

15 $HOOH \rightarrow 2\dot{O}H$

16 $\dot{O}H + C_3H_6 \rightarrow H_2O + CH_2{=}CH\dot{C}H_2$

17 $CH_2{=}CHCH_2O\dot{O} \rightsquigarrow$ chain stop

Reaction (17) is postulated, because a wall effect was observed in our previous work; the oxidation reaction took place above 300°C with the reactor 56.3 mm in i. d.[1] and at 360°C with the reactor

24.5 mm in i. d.[2),*4] This strongly indicates the prolonged induction period for the 24.5 mm reactor discussed in Exp. A_0 of the previous paper.[2)] The surface area-to-volume ratios of these reactors differ by a factor of about 2.3. Hence, the wall effect of these stainless steel reactors may be evaluated as stronger than that of the entire surface of the fluidizing particle (silicon carbide).[*5] The induction period of a radical-chain reaction ends when a sufficient quantity of the branching agent is accumulated.[6)] The branching agent of this reaction is acetaldehyde (AA), which, it has been proposed, is formed from the allyl peroxy radical.[2)] Thus, the prolonged induction period can be attributed to the reduced rate of the accumulation of AA. The peroxy radical is considered to be decomposed rapidly on the metallic surface, according to the discussion of Walsh *et al.*[7)] This must be the cause of the prolonged induction period with the reactor 24.5 mm in i. d. Therefore, reaction (17) is reasonable.

In the propylene-excess atmosphere under pressure, the probability of the encounter of radicals with propylene is very high, and propylene is assumed to react easily with radicals in the following two ways: the addition of radicals to the double bond, or the abstraction of hydrogen by radicals. Both these reactions produce other radicals. Therefore, the termination reactions in the gas phase is not considered here.

The following equations are obtained on the assumption of the stationary state of the concentrations of radicals. It is postulated that the stationary-state approximation can hold for the concentrations of peroxide molecules. In the initial step of the reaction, the concentrations of propylene and oxygen can be considered to be constant, the following kinetic equations are derived on this assumption.[*6]

In the following equations, the suffix of the rate constant k indicates a reaction described above, P, O, AA, PO, and C=C indicating propylene, oxygen, acetaldehyde, propylene oxide, and ethylene respectively.

The concentrations of main radicals are as follows:

$$[\mathrm{CH_2{=}CH{-}CH_2{-}O{-}\dot{O}}] = 3[\mathrm{O}](k_0[\mathrm{P}] + k_{4a}[\mathrm{AA}])/k_{17} \tag{1}$$

$$[\mathrm{CH_3{-}\dot{C}{=}O}] = k_{4a}[\mathrm{AA}][\mathrm{O}]/G \tag{2}$$

$$[\mathrm{CH_2{=}CH{-}\dot{C}H_2}] = 3F(k_0[\mathrm{P}] + k_{4a}[\mathrm{AA}])/k_1\cdot k_{17} \tag{3}$$

where

$$G \equiv k_{4b}[\mathrm{O}] + k_{5b}[\mathrm{P}] + k_{5a}$$

$$F \equiv (k_{2a} + k_{2c})[\mathrm{P}] + k_{2d} + k_{2f} + k_{17}$$

The concentrations of these radicals are positive functions of the concentration of AA, which was previously concluded to be the degenerate branching agent in this reaction.[2)]

The rate of formation and the concentration of AA are as follows:

$$\frac{\mathrm{d}}{\mathrm{d}t}[\mathrm{AA}] \equiv r_{\mathrm{AA}} = \chi[\mathrm{P}][\mathrm{O}] + \varphi[\mathrm{AA}] = \chi[\mathrm{P}][\mathrm{O}]\exp(\varphi t) \tag{4}$$

$$[\mathrm{AA}] = \omega[\exp(\varphi t) - 1] \tag{5}$$

where

$$\varphi \equiv k_{4a}[\mathrm{O}][(3k_{2d}/k_{17}) - (k_{4b}[\mathrm{O}] + k_{5a})/G] \tag{6}$$

$$\chi \equiv 3k_0\cdot k_{2d}/k_{17} \tag{7}$$

$$\omega \equiv \chi[\mathrm{P}][\mathrm{O}]/\varphi$$

Eqs. (4) and (5) show that the rate of the increase of AA is accelerated with the reaction time, and that the accumulations of the allyl, allyl peroxy and acetyl radicals are also accelerated with the reaction time, as may be seen from Eqs. (1)—(3).

Equations (8)—(11) are derived for O, PO, CO, and C=C respectively:

$$-\frac{\mathrm{d}}{\mathrm{d}t}[\mathrm{O}] \equiv r_{\mathrm{O}} = \alpha[\mathrm{O}] + \gamma\cdot\omega(\mathrm{e}^{\varphi t} - 1)[\mathrm{O}] = \alpha[\mathrm{O}] + \gamma[\mathrm{AA}][\mathrm{O}] \tag{8}$$

$$\frac{\mathrm{d}}{\mathrm{d}t}[\mathrm{PO}] \equiv r_{\mathrm{PO}} = \beta[\mathrm{P}]^2[\mathrm{O}] + \delta\cdot\omega(\mathrm{e}^{\varphi t} - 1)[\mathrm{O}] = \beta[\mathrm{P}]^2[\mathrm{O}] + \delta[\mathrm{AA}][\mathrm{O}] \tag{9}$$

$$\frac{\mathrm{d}}{\mathrm{d}t}[\mathrm{CO}] \equiv r_{\mathrm{CO}} = \theta[\mathrm{P}][\mathrm{O}] + \eta\cdot\omega(\mathrm{e}^{\varphi t} - 1)[\mathrm{O}] = \theta[\mathrm{P}][\mathrm{O}] + \eta[\mathrm{AA}][\mathrm{O}] \tag{10}$$

[*4] The apparent reaction time is 21 sec for the experiment using the 56.3 mm reactor[1)] and 8 sec for that with the 24.5 mm reactor.[2)] It was confirmed further that the results of the reaction experiment with the 24.5 mm reactor varied only a little in the range of the apparent reaction time from 5 to 15 sec. This result indicates that the variation in the apparent reaction time in this order does not significantly affect the results of the reaction experiments using the fluidized bed reactor. Therefore, the above discussion about the length of the induction period is not disturbed by the variation in the apparent reaction time.

[*5] A detailed discussion of the effect of several kinds of fluidizing particles will be published later.

6) N. N. Semenov, "Some Problems in Chemical Kinetics and Reactivity," Japanese translation by T. Kwan and A. Matsuda, Vol. 2, Chap. 12, Iwanami Shoten Co., Tokyo (1964).

7) D. E. Cheaney, D. A. Davis, A. Davis, D. E. Hoare, J. Prothesroe and A. D. Walsh, "Seventh Symposium (International) on Combustion (1958)," Butterworths Sci. Pub., London (1959), p. 183.

[*6] In the derivation of these rate equations, the rate of the formation of the hydroxy radical was regarded as being first-order with regard to the concentration of hydrogen peroxide, considering the initial step of the reaction.

$$\frac{\mathrm{d}}{\mathrm{d}t}[\mathrm{C{=}C}] \equiv r_{\mathrm{C=C}} = \varepsilon[\mathrm{P}][\mathrm{O}] + \zeta\cdot\omega(\mathrm{e}^{\varphi t} - 1)[\mathrm{O}]$$

$$= \varepsilon[\mathrm{P}][\mathrm{O}] + \zeta[\mathrm{AA}][\mathrm{O}] \quad (11)$$

where:

$\alpha \equiv k_0[\mathrm{P}] + (3\,k_0\cdot F[\mathrm{P}])/k_{17}$

$\beta \equiv 3k_0\cdot k_{2\mathrm{a}}\cdot k_{6\mathrm{a}}/k_{17}(k_{2\mathrm{b}} + k_{6\mathrm{a}})$

$\gamma \equiv k_{4\mathrm{a}}(1 + k_{4\mathrm{b}}[\mathrm{O}]/G + 3F/k_{17})$

$\delta \equiv k_{4\mathrm{a}}[3k_{2\mathrm{a}}\cdot k_{6\mathrm{a}}[\mathrm{P}]/k_{17}(k_{2\mathrm{b}} + k_{6\mathrm{a}}) + k_{4\mathrm{b}}[\mathrm{O}]/G]$

$\varepsilon \equiv \frac{3k_0}{k_{17}}(k_{2\mathrm{f}} + k_{2\mathrm{a}}[\mathrm{P}])$

$\zeta \equiv \frac{3k_{4\mathrm{a}}}{k_{17}}(k_{2\mathrm{f}} + k_{2\mathrm{a}}[\mathrm{P}])$

$\eta \equiv k_{4\mathrm{a}}(3k_{2\mathrm{f}}/k_{17} + k_{5\mathrm{a}}/G)$

$\theta \equiv 3k_0\cdot k_{2\mathrm{f}}/k_{17}$

As has been shown above, an exponential term or the concentration of AA is present in all kinetic equations. Therefore, these equations may be considered to accord well with the results of the previous work[2] in which AA was demonstrated to be the branching agent in this reaction; also, the relations between the concentration of AA and the reaction rates for O, PO, CO, and C=C can be obtained from the reaction scheme discussed in that earlier paper.[2] The values of α, β, γ, δ, ε, ζ, η, θ, and χ should be positive. As has been shown by Semenov,[6] the reaction rates described above are subject to the value of φ, which can be either positive or negative.

These rate equations represent the well-known "S-shaped rate-*vs.*-time curves" which are characteristic of a degenerate branching reaction, if the value of φ is positive and relatively small, as has been described by Semenov.[6]

The reaction scheme described above can not be a full and precise description of a "perfect reaction mechanism," however, a complete elucidation of such a mechanism is impossible at present. The scheme described above should thus be considered as a description of the predominant course of the homogeneous gas-phase oxidation of propylene in a propylene-excess atomsphere under pressure. Therefore, if the kinetic equations here derived fit the experimental results well, the reaction scheme presented certainly obtains experimental support.

Results

Residence-time Distributions. Figure 2 shows the standard curves of the residence-time distribution function for the Peclet-Bodenstein numbers of 50 and 100; in the figure these curves are compared with the experimental results at the reaction times of 1.1 and 0.3 sec. Their Peclet-Bodenstein numbers are evaluated from Fig. 2 as 70 and 90. On the basis of these values, the residence-time (reaction-time) distribution can be practically neglected under the conditions of the kinetic experiments described below. Thus, the reaction time in this reactor can be easily calculated on the basis of the plug flow.

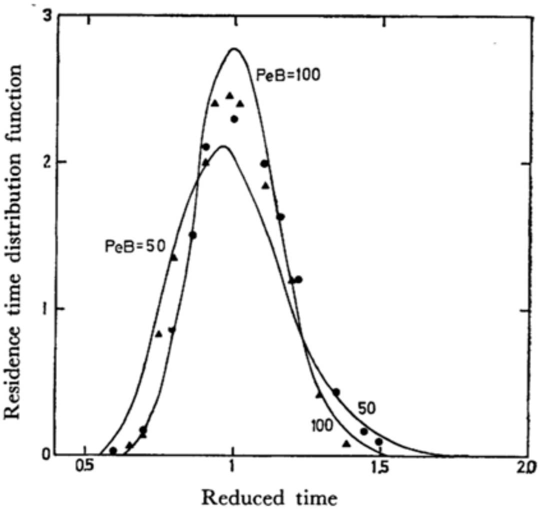

Fig. 2. Results of the measurement of residence time distribution.
▲ 1.1 sec ● 0.3 sec PeB, Peclet-Bodenstein no.

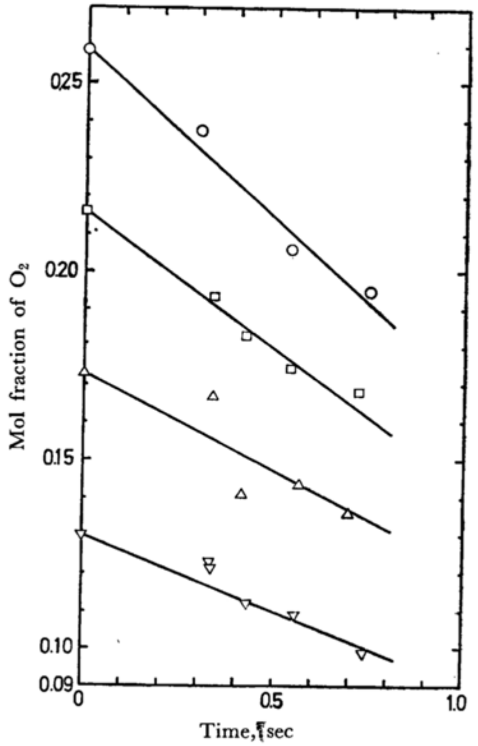

Fig. 3. Effect of the mol ratio (O_2/C_3H_6) on the comsumption of O_2 *vs.* reaction time correlation at 385°C under 3 atm.
○, O_2 0.26/C_3H_6 0.70 □, 0.22/0.74
△, 0.17/0.78 ▽ 0.13/0.82

The Effect of the Molar Ratio of Propylene to Oxygen. Experiments were carried out at 385°C, under 3 atm and with reaction times of 0.3—0.75 sec. The molar ratios of oxygen to propylene examined were 0.26/0.70, 0.22/0.74, 0.17/0.78, and 0.13/0.82; here, the molar fraction of propylene was regarded as roughly constant. The reaction rates were determined from the gradients of the straight lines shown in Figs. 3—5. The reaction order was determined from the gradients of plots, log (molar fraction of oxygen) *vs.* log (rate); Fig. 6 shows the plot of the rate of the comsumption of oxygen and the rates of the

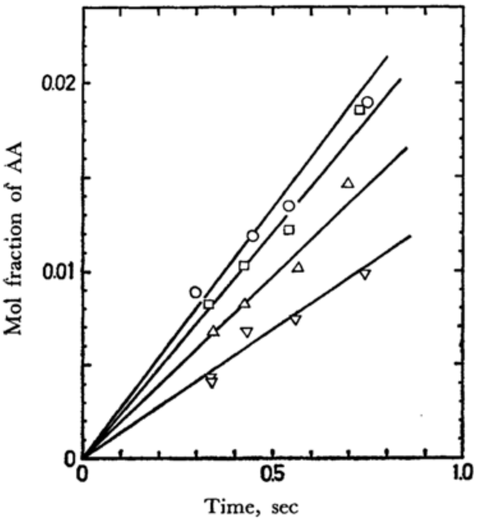

Fig. 4. Effect of the mol ratio (O_2/C_3H_6) on the yield of AA *vs.* reaction time correlation at 385°C under 3 atm.
○, O_2 0.26/C_3H_6 0.70 □, 0.22/0.74
△, 0.17/0.78 ▽, 0.13/0.82

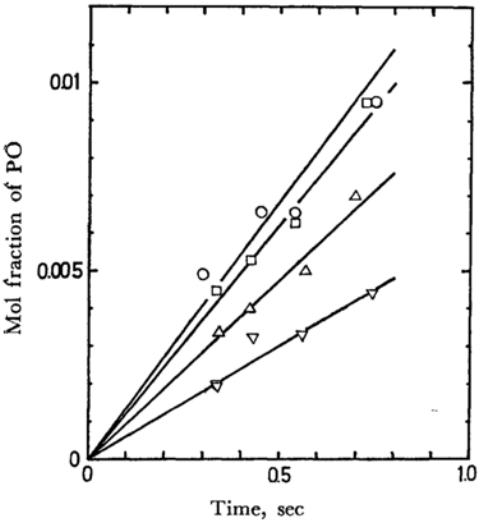

Fig. 5. Effect of the mol ratio (O_2/CH_6) on the yield of PO *vs.* reaction time correlation at 385°C under 3 atm.
○, O_2 0.26/C_3H_6 0.70 □, 0.22/0.74
△, 0.17/0.78 ▽, 0.13/0.82

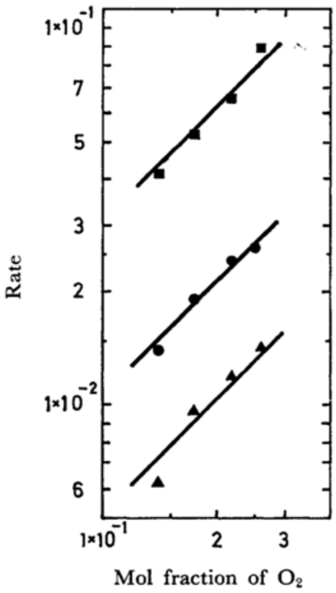

Fig. 6. Logarithmic plot; mol fraction of O_2 *vs.* the rate of the comsumption of O_2 (■) and the rate of the formation of AA (●) and PO (▲).

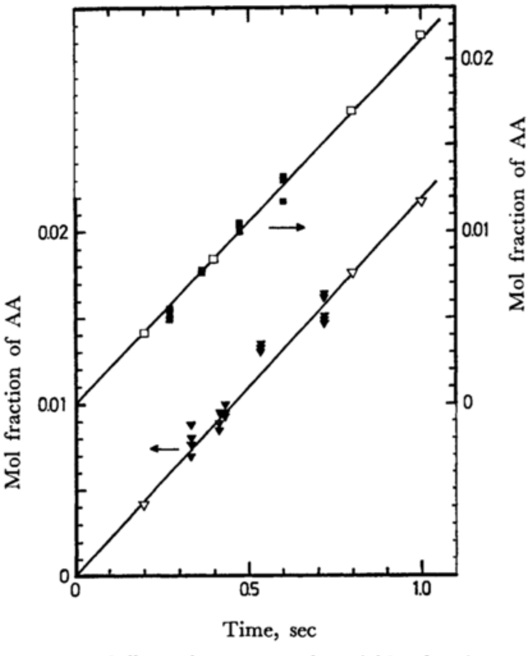

Fig. 7. Effect of temp. on the yield of AA *vs.* reaction time correlation at O_2 0.22/C_3H_6 0.74 under 3 atm.
■, measured at 374°C □, calc. from Eq. (5) for 374°C ▼, measured at 384°C ▽, calc. from Eq. (5) for 384°C

Table 1. Rate constants at 385°C under 3.0 atm

$-\frac{d}{dt}[O_2]=k_O[O_2]$	$\frac{d}{dt}[AA]=k_{AA}[O_2]$	$\frac{d}{dt}[PO]=k_{PO}[O_2]$
k_O, sec^{-1}	K_{AA}, sec^{-1}	k_{PO}, sec^{-1}
0.34	0.12	0.082

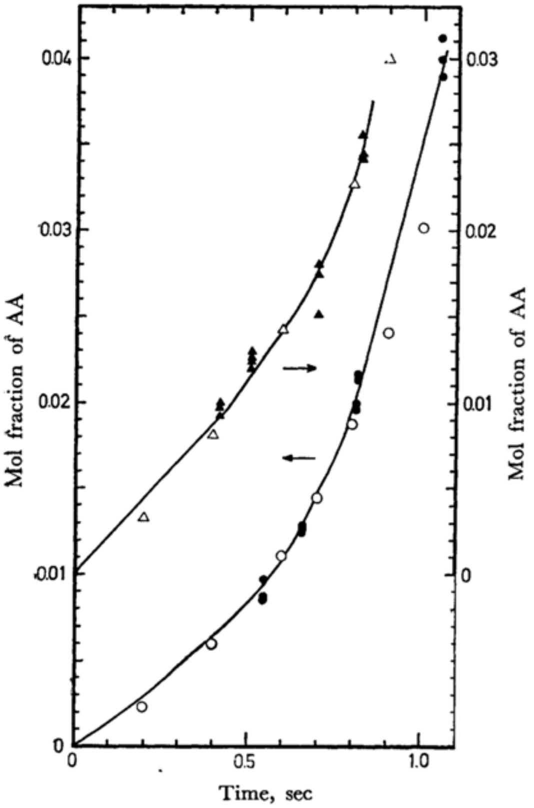

Fig. 8. Effect of temp. on the yield of AA *vs.* reaction time correlation at O_2 0.22/C_3H_6 0.74 under 3 atm.
▲, measured at 399°C △, calc. from Eq. (5) for 399°C ●, measured at 421°C ○, calc. from Eq. (5) for 421°C

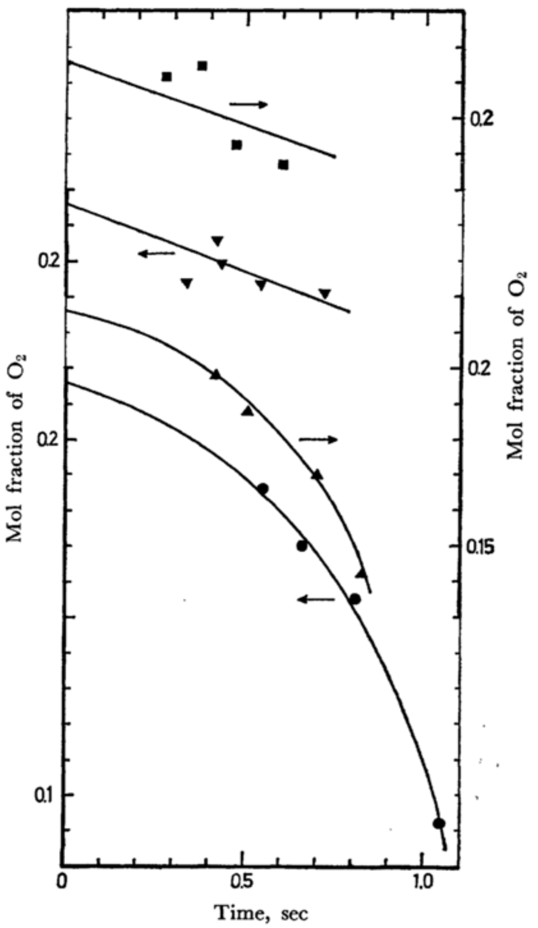

Fig. 9. Effect of temp. on the consumption of O_2 *vs.* reaction time correlation at O_2 0.22/C_3H_6 0.74 under 3 atm.
■, 374°C ▼, 384°C ▲, 399°C ●, 421°C

formation of AA and PO. The rate equations and rate constants obtained are shown in Table 1.

Effects of Temperature. Experiments were carried out under the following conditions: 3 atm, molar ratio of 0.22/0.74 (oxygen/propylene), and temperatures of 374, 384, 399, and 421°C. The results for AA are shown in Figs. 7 and 8, and those for O, PO, CO and C=C, in Figs. 9, 10 11 and 12 respectively. Equations (4)—(5) and (8)—(11) were applied to these results; the constants in these equations were determined using the observed values of molar fractions or the rates at the short reaction times measured at the two points which have different gradients on each curve. The concentration-*vs.*-time curves for AA are shown in Figs. 7 and 8; here the black points represent observed values and the open points represent values calculated using Eq. (5). Table 2 contains the constants in Eqs. (4)—(5) and (8)—(11). The observed and calculated concentrations of AA and rates are compared with each other in Table 3.

Discussion

On the Reaction Scheme. As is shown in Figs. 7 and 8, excellent agreements are obtained between the observed and calculated values for the concentration of AA. The small deviations

TABLE 2. CONSTANTS IN RATE EQUATIONS

Temp. °C	φ	ω	$\alpha(\times 10^{-1})$*	$\beta(\times 10^{-2})$*	γ*
374	0.020	1.1	1.7	9.2	
384	0.020	1.0	1.8	10	
399	1.5	0.0098	0.60	0.085	35
421	1.9	0.0051	1.4	3.3	32

Temp. °C	δ*	$\chi(\times 10^{-2})$	ε*$(\times 10^{-2})$	ζ*	θ*$(\times 10^{-2})$	η*
374		13	3.3		30	
384		14	2.4	3.4	29	
399	5.1	9.3	2.8	1.6	5.7	20
421	5.1	6.2	0.61	2.8	11	15

* Owing to the straight lines in concentration *vs.* time plots for O, PO, CO and C=C at 374 and 382°C as shown in Figs. 8—11, the values of α and γ, β and δ, θ and η, ε and ζ, can not be obtained separatly as seen from Eqs. (8)—(11).

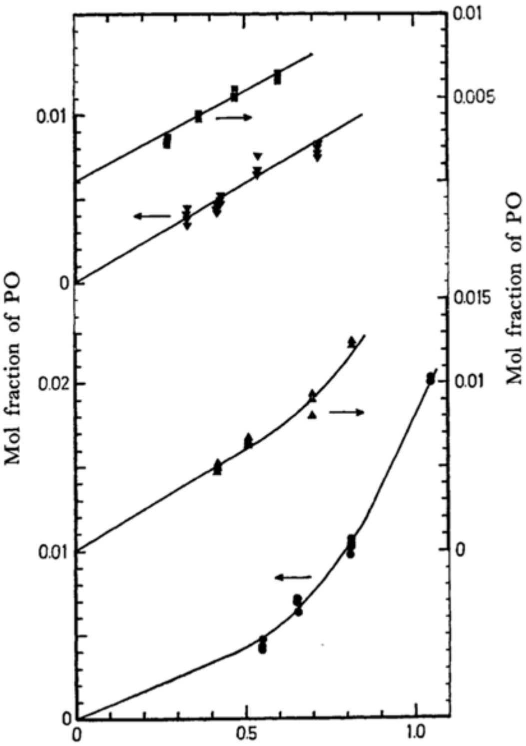

Fig. 10. Effect of temp. on the yield of PO *vs.* reaction time correlation at O_2 0.22/C_3H_6 0.74 under 3 atm.
■, 374°C ▼, 384°C ▲, 399°C ●, 421°C

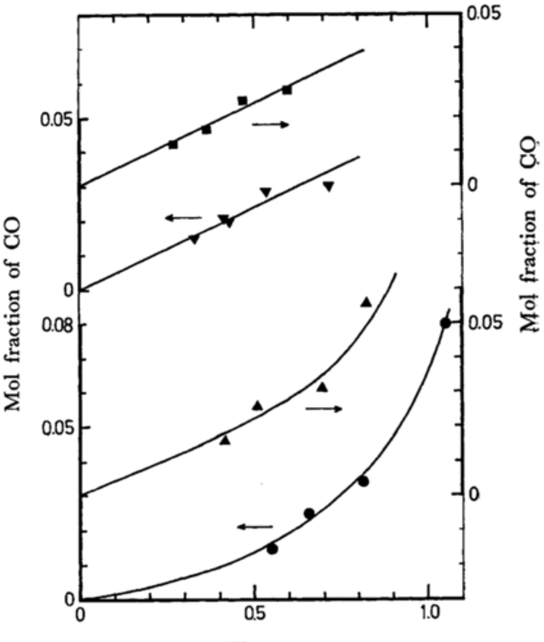

Fig. 11. Effect of temp. on the yield of CO *vs.* reaction time correlation at O_2 0.22/C_3H_6 0.74 under 3 atm.
■, 374°C ▼, 384°C ▲, 399°C ●, 421°C

which are observed in Fig. 8 at the longer reaction time can be ascribed to the failure of the postulation of the initial reaction step. Therefore, it may be concluded that Eq. (5) is suitable for describing the course of the change in the concentration of AA *vs.* the reaction time in the initial step of this reaction system.

As is shown in Table 3, the agreements between the observed and calculated values of r_O, r_{AA}, r_{PO}, r_{CO} and $r_{C=C}$ are satisfactory. It may be concluded, therefore, that Eqs. (4), (8), (9), (10) and (11) are quite satisfactory for describing the reaction rates in this reaction system for O, PO, AA, CO, and C=C. The first order rate equations obtained experimentally for O, AA and PO (Table 1) support this conclusion, because the exponential

TABLE 3. COMPARISON OF OBSERVED VALUES WITH THE CALCULATED VALUES

Conc. and rates	Reaction time sec	374°C		384°C		399°C		421°C	
		Obs.	Calc.	Obs.	Calc.	Obs.	Calc.	Obs.	Calc.
$[CH_3CHO]^*$ $(\times 10^{-2})$	0.3	0.64	0.64	0.67	0.62	0.66	0.56	0.46	0.40
	0.5	1.1	1.1	1.1	1.1	1.1	1.1	0.82	0.83
	0.8	—	1.7	1.8	1.8	2.3	2.3	2.0	1.9
$-\frac{d}{dt}[O_2]^{**}$ $(\times 10^{-2})$	0.3	3.6	3.6	3.8	3.8	5.5	5.5	6.0	5.8
	0.5	3.6	3.6	3.8	3.8	9.5	9.5	8.8	8.8
	0.8	3.6	3.6	3.8	3.8	23	18	16	16
$\frac{d}{dt}[CH_3CHO]^{**}$ $(\times 10^{-2})$	0.3	2.1	2.1	2.2	2.2	2.2	2.5	1.8	1.8
	0.5	2.1	2.1	2.2	2.2	2.9	3.0	2.1	2.6
	0.8	2.1	2.1	2.2	2.2	6.7	4.9	5.2	4.6
$\frac{d}{dt}[CH_3\overset{O}{CHCH_2}]^{**}$ $(\times 10^{-2})$	0.3	1.1	1.1	1.2	1.2	1.2	0.62	0.83	0.83
	0.5	1.1	1.1	1.2.	1.2	1.2	1.2	0.90	1.3
	0.8	1.1	1.1	1.2	1.2	2.5	2.5	2.4	2.5
$\frac{d}{dt}[CO]^{**}$ $(\times 10^{-2})$	0.3	5.0	5.0	4.6	4.6	3.3	4.7	3.2	2.6
	0.5	5.0	5.0	4.6	4.6	5.6	5.2	4.6	4.8
	0.8	5.0	5.0	4.6	4.6	11	14	8.0	9.2
$\frac{d}{dt}[C_2H_4]^{**}$ $(\times 10^{-3})$	0.3	5.3	5.3	8.8	5.8	6.5	6.9	3.4	3.7
	0.5	5.3	5.3	12	11	8.3	8.0	6.2	5.5
	0.8	5.3	5.3	—	—	12	14	12	16

* expressed in mol fraction ** expressed in (mol fraction)/(sec)

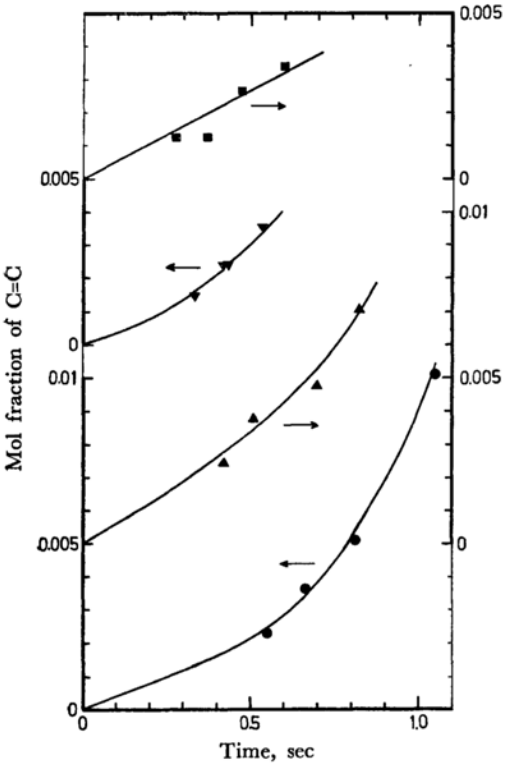

Fig. 12. Effect of temp. on the yield of C_2H_4 *vs.* reaction time correlation at O_2 0.22/C_3H_6 0.74 under 3 atm.
■, 374°C ▼, 384°C ▲, 399°C ●, 421°C

terms in Eqs. (4), (8) and (9) are not so large; when φt is small, as is shown in Table 2, these equations apparently become first-order rate equations. Thus all the kinetic equations derived have been proved to fit the experimental results.

Though many reaction schemes leading to the same rate equations are plausible, the authors' scheme has been supported by experiments and also by the results of many other authors' cited in the previous paper.[2] It seems, therefore, reasonable to conclude that the reaction scheme presented in this paper is a correct description of the main course of this reaction. In consideration of the values of the reaction rate constants (Tables 1 and 2) and the yields of the various oxidation products given in Figs. 4—6 of the previous paper,[2] the relative weight of the reaction paths may finally be considered to be as follows:

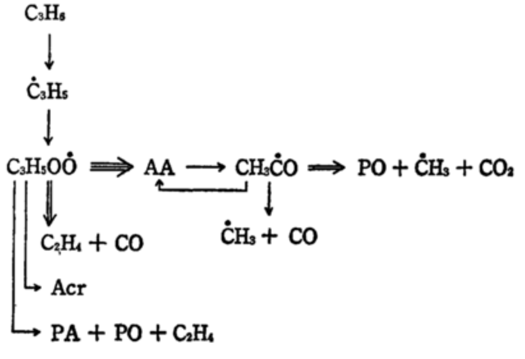

On the Slow Rate Period. From the above discussions, the characteristics of this reaction system can be represented in terms of the behavior of AA. In Fig. 8, for AA at 399 and 421°C a steep increase in AA formation is observed after a linear increase. This linear sector corresponds to the constant-reaction-rate region at the initial reaction time. As is shown in Fig. 7 for AA at 374 and 384°C, this linear sector continues to the end of the experiment; in this case, the values of φ are small, as shown in Table 2. The value of φ undergoes a sudden increase at some temperature between 384 and 399°C, as is also shown in Table 2.

In Eq. (4), the values of $\chi(\equiv 3k_0 \cdot k_{2d}/k_{17})$ decrease slowly with the rise of temperature, as shown in Table 2. Therefore, the $3k_{2d}/k_{17}$ term, in φ may also be considered to change slowly; moreover, it is reasonable to consider that $k_{4a}[O]$ the term in φ changes slowly. Thus, the sudden increase in φ may be attributed to the sudden decrease in the $(k_{4b}[O]+k_{5a})/(k_{4b}[O]+k_{5b}[P]+k_{5a})$ term in Eq. (6). Here, this term of φ may be written as $a/(a+k_{5b}[P])$. Therefore, the value of φ can increase rapidly upon the gradual increase in k_{5b} with the temperature. Thus, the difference between the kinetic curves of 374 and 384°C and those of 399 and 421°C can be reasonably explained.

The authors are indebted to Mr. Mitsuhiko Iwasaki for his advices on the pulse tracer technique and for his kind help for the digital computer calculation, also thank Nippon Petrochemicals Co., Ltd, for supplying the propylene gas.